DOI: 10.13009/EUCASS2023-807
Aerospace Europe Conference 2023 – 10TH EUCASS – 9TH CEAS

Analysis of an arc heated air plasma generator for material screening applications

Mathilde Ridard†, Bruno Van-Ootegem*, Grégory Pinaud*, Kevin Haras**
** ArianeGroup*
Les cinq Chemins, 33185 Le Haillan, France
mathilde.ridard@ariane.group
† Corresponding Author

Abstract

ArianeGroup is operating an arc heated air plasma generator to test Ceramic Matrix Composites (CMC) and phenolic composites in rocket nozzle and / or atmospheric re-entry environments. This torch is able to produce an oxidizing flow with temperatures of up to 4000K, heat fluxes of up to 6 or 7 MW/m^2 and shear values of about 500 Pa. By its design, the reliability and reproducibility of the torch have been thought to be compatible with the material screening needs.

In order to predict the thermal and erosive behaviour of any known material exposed to the extreme conditions of the plasma torch, complex coupled fluid-solid simulations are needed. The analysis logic adopted in this article is incremental and covers the first steps required for this approach.
First, CFD calculations of the external plasma jet discharging into the laboratory's ambient air are conducted. Two types of configurations are tested: the free jet configuration and an ablation test configuration with a sample holder positioned into the plasma flow.
The choices of turbulence models and the assumptions of the jet inlet boundary conditions are discussed by means of a sensitivity study and a comparison with the experimental calibration measurements, available only at a reasonable distance from the potential core along the jet axis.
Finally, an estimation of the fluxes in the potential core is conducted via a simplified thermal modelling of the solid sample thermal behaviour, as well as a comparison with temperature measurements from sacrificial tests of Carbon-Carbon composites.
In further development, the energy balance at the surface of the sample can be completed to take into account the effects of the ablation of the material and thermochemical coupling with the oxidizing environment, always with the aim of constructing a coupled complex simulation.

1. Introduction

Plasma torches have been operated in the aerospace industry for the past decades for several applications, such as plasma spray processes for production of high performance (metallic or ceramics) coatings ([3]), nanopowder production [2][18], as well as waste treatment, arc welding, and plasma cutting. It can also be operated as a material screening testing facility regarding thermochemical resistance of materials.

Plasma torches are able to produce very high-temperature, high-velocity oxidizing flows. Therefore, they allow to test extreme conditions of convection and chemical oxidation simultaneously on the surface of a material representative atmospheric re-entry or rocket nozzle environments.

In particular, these extreme conditions are interesting to test material resistance to ablation, which is due both to thermochemical erosion (which results from a competition between chemical reactions and gaseous diffusion through the porous carbon-based material), and mechanical effects (as shear stress and particle impacts may increase the erosion of a material surface that is made more fragile due to thermochemical erosion).

In the context of laboratory material screening applications, those extreme conditions are closer to the real re-entry or rocket nozzle conditions than the one produced by other devices, such as Thermo-Gravimetric Analysis that can test only chemical oxidations effects with minimal convective or diffusive effects. However, as the physics are strongly

DOI: 10.13009/EUCASS2023-807

coupled in such extreme conditions, it is even more difficult to build a comprehensive ablation model of materials in a torch environment.

As a first step, it is therefore necessary to characterize properly the flow fields generated by the plasma torch in terms of thermal, aerodynamics, turbulent, chemical and shear stress conditions.
ArianeGroup arc heated air plasma torch facility can be modulated in order to reach various specifications. It is able to produce an oxidizing flow with heat fluxes up to 6MW/m^2 and shear stresses of about 500Pa. The electrical power of the plasma torch is 750kW.

Experimental campaigns have been performed to test several composite materials and several torch operating conditions. For some tests, a laser device has been added in order to locally increase the samples surface temperature without additional convective flow. Calibration tests have also been performed.

In order to predict the thermal and erosive behavior of a material placed in the extreme conditions of a plasma torch, a coupled simulation is needed to model the aerodynamic, thermal and chemical properties of the flow, as well as its interaction with the solid material samples exposed to the extreme torch environment. The objective is to find predictable models allowing to compare the thermochemical behavior of different materials under the torch conditions, and in the future be able to extrapolate their behavior to a wide range of extreme thermochemical and convective conditions. Such a comprehensive approach is a long term objective since the physical phenomena behind those problems are complex. Therefore, numerical models of plasma torches often consider the different physics involved as separated, as described in the following part.

2. Literature review

Studies of the plasma flow inside of a torch have to take into account the coupling between electromagnetic fields and the Navier Stokes fluid dynamics equation, as it was proposed by Takali [1].
Outside of the plasma torch, the effects of electromagnetic fields on the external jet are usually neglected, and the plasma jet is often referred to as “thermal” plasma jet, which means that the electrons and the heavy particles of the plasma are supposed to be at the same temperature.

In a numerical simulation of an external plasma torch thermal jet, it is necessary to model properly turbulence effects. The plasma jet of a torch is a high-velocity, high-temperature flow exiting from the nozzle. As stated by Shigeta [3], the external jet is divided into two main zones: the high-velocity, high-temperature core right after the exit of the torch, and an intermediate zone between the plasma core and the cold ambient gas. These interfacial regions have lower temperature and lower velocities, and have been proved to be more turbulent than the potential core: in fact, multi-scale eddies are forming and developing in those regions, causing the plasma to entrain cold ambient air at its fringe. Temperatures and velocities then rapidly decrease as one moves away from the exit along the central axis. In this context, it appears that the aerothermal fluxes calculated on a probe or a sample placed in the plasma jet, are then strongly influenced by the precision of the turbulence model.

Different turbulent models have been adopted to simulate the gas fields of round jets (either for plasma torch jets or reactive ramjets for instance). Most of them are based on the Finite Difference Method (FDM) with Reynolds Average Navier-Stokes equations (RANS). The most commonly used model is the well-known two equations k-epsilon model proposed by Launder et al ([4]). However, in the context of round turbulent jets, the standard k-epsilon model has shown some limitations. Over the years several authors such as Launder [5], McGuirk [6], Morse [7], Pope [8] and Turpin & Troyes [9] have then proposed to modify its associated set of constants ($C_{1\epsilon}$, $C_{2\epsilon}$, C_μ, σ_k and σ_ϵ) to achieve better numerical predictions. Turpin & Troyes [9] in particular compare their new set of turbulent parameters with the standard k-epsilon model for reacting and non-reacting turbulent flows, with two validation cases (“low Mach number flame” and “supersonic non-reacting” flows). Bolot [10] compares the standard k-epsilon model with the Reynolds Stress Model (RSM) of the commercial software FLUENT and the Chen-Kim k-epsilon model of the PHOENICS CFD code: these two provides longer potential cores than the standard k-epsilon model. In parallel, other turbulence models have been implemented in commercial software such as ANSYS FLUENT to overcome the well-known limitations of the standard k-epsilon analysis. One of them is the Realizable k-epsilon model. This model has been developed as a new k-epsilon eddy viscosity model with a new dissipation rate equation and a new realizable eddy viscosity formulation, and have been proved to remove the “well-known spreading rate anomaly of planar and round jets” [11].

DOI: 10.13009/EUCASS2023-807

Apart from FDM, Lattice Boltzman Method (LBM) is being investigated as wall to model the plasma flow fields. For instance, according to [11], this method exhibits some advantages compared to the classical approaches with finite difference methods. In particular, the LBM approach was found more efficient and simpler to use, and was able to comply both with experimental results and previous numerical results.

Furthermore, the correct modelling of turbulence effects is important in the case of reacting flows such as plasmas. In the high temperature potential core, the chemical reactions occur prior to turbulent mixing due to smaller characteristic time steps, whereas in the far field, temperatures are lower and the time scale for temperature equilibration is faster than the time step for turbulent mixing. In these conditions, the standard k-epsilon approaches (which already show some limitations for round turbulent jets) are expected to perform poorly in the high temperature potential core and are rather recommended for the far field zones only ([16], [17]). Turpin and Troyes [9] also remind that a correct prediction of the turbulent values k and epsilon is necessary to predict properly some characteristics of the flow such as turbulent viscosity, as well as chemical reactions, since the reaction rates are directly estimated from the values of k and epsilon.

Data of experimental studies are available for different plasma torch configurations, such as plasmas of pure argon [18], air and argon ([13]), pure nitrogen [19], or CO2/N2/air ([15]).

Other studies have been conducted to investigate specifically the gas-surface interactions of a composite sample in a certain plasma jet environment for specific torch configurations (such as the Plasmatron of the Von Karman Institute generating air / argon plasmas on a 3D Carbon-Carbon material, [13], [14]). Those studies show the need for complex coupled fluid-solid simulations accounting for thermochemical effects.

3. Experimental set-up

ArianeGroup arc heated air plasma torch can be set at multiple operating points, each one being characterized by a value of intensity and air mass flow rate, defining a value of electrical power range going from 200kW to 750 kW. The plasma exits the torch through a several hundred millimeter long tubular canal with its own cooling circuit, at atmospheric pressure. The torch is able to produce an oxidizing flow with temperature of 4000K, heat fluxes of up to 6 MW/m^2 and shear values of about 500Pa. In those operating conditions, the external flow is subsonic.
By its design, the reliability and reproducibility of the torch have been demonstrated to be compatible with the material screening needs.

A photo of the plasma generator and of the external plasma jet is provided in Figure 1 below.

Figure 1 : Arc heated air plasma generator

Two different configurations of experimental installation can be placed into the torch plasma jet.

Firstly, calibration devices (pressure probe and flux probes) may be used to perform measurements and characterizations in the flow fields, with their own specific cooling circuit.
Due to the extreme temperatures into the plasma jet, especially into its potential core, calibration tests cannot be carried out too close from the nozzle exit, as there would be a risk of serious damage to the measuring device. For instance, the heat probes are typically designed for fluxes of $5MW/m^2$ maximum. Taking these limitations into account, the calibration tests made it possible to measure constantly decreasing values of heat fluxes, temperatures and velocities along the central axis, over the range of distances considered.

DOI: 10.13009/EUCASS2023-807

Secondly, for screening material applications, a sample carrier device can be positioned into the flow field, and the distance between the exit and the sample can be modulated in order to test different flow conditions for the same operating point of the torch. A spectroradiometer, pyrometers and thermocouples are then used to measure the evolution of surface and material temperature of the sample during the test. Cameras are filming the surface recession from different angles. Initial and final geometry of the sample are scanned before and after the test to evaluate the total surface recession.

4. Analysis logic

To fully represent an ablation test on a composite material, it would be necessary to perform an unsteady, fluid-solid coupled modelling between the hot plasma jet, the ambient air driven by it, and the material sample. This simulation should take into account the complexity of the physical phenomena involved, including turbulent mixing, thermochemical reactions into gaseous phases and with carbon at the material surface, diffusion of oxidizing species through the material boundary layer, radiative exchanges or even thermal conduction into the sample.

Such a complete simulation is set as a long term objective. In this paper, an incremental approach is rather adopted. Estimates are first conducted by decoupling these phenomena and by proposing simplified models.

This study is then focused on modelling the external jet of the torch at one specific operating point only, with the help of some experimental measurements. In this objective, CFD simulations have been performed on the external plasma torch jet.

An assumption of local thermodynamic equilibrium is made for the external plasma jet, meaning that electrons and heavy particles are at the same temperatures, which is valid in the absence of electric or electromagnetic field ([17], [20]). The plasma is treated as a compressible and turbulent flow. The jet is assumed to be axisymmetric (round jet) and the simulation is steady. A simplification here is that the chemical reactions are not explicitly modelled in the CFD simulation. Instead, the air plasma flow and the surrounding air properties, such as viscosity, heat capacity and thermal conductivity, are tabulated as functions of temperatures, with peaks accounting for the dissociation and chemical reactions of the air plasma at high temperatures. This approach is similar to the one adopted by Bolot [10] for their numerical studies of turbulence of an argon-hydrogen plasma mixture.

Regarding boundary conditions, the surrounding air is injected with a small (non-zero) velocity (to help with convergence), at atmospheric pressure and room temperature.

The plasma jet is known to be discharging into the cold ambient of the laboratory at atmospheric pressure, through a 35mm diameter exit canal, but the velocity and enthalpy (or temperature) profiles are not known precisely since no measurements are available right after the exit (as probe devices would not survive the extreme thermal conditions in the potential core at these operating conditions). Therefore, assumptions will have to be made regarding the velocity and temperature profile forms as discussed in the following sections. The external plasma jet will be simulated with several turbulence models available in the commercial code ANSYS FLUENT, and with two assumptions of profiles forms at the hot plasma inlet. Besides, two configurations of the experimental set-up will be modelled with CFD approaches: the first one is the free jet alone, whose velocity and temperature fields will be compared to the experimental probe measurements available along the axis far from the exit; the second one is very similar to a real ablation test configuration, with the same sample carrier device exposed to turbulent, moderate-temperature intermediate region of the plasma jet, except that the material sample is replaced by a heat probe.

Lastly, a simplified heat flux analysis is performed on a third experimental set-up, which happens to be a real ablation test configuration, on a sample of CMC, exposed to the high-temperature potential core. This analysis is based on simple energy balance considerations and experimental temperature measurements from ablation tests performed with the plasma generator.

DOI: 10.13009/EUCASS2023-807

4.1 Free jet simulations with flat profiles (mean values) at the inlet boundary of the torch

The first configuration to be modelled in CFD is the free external plasma jet.

In the first simulations, hot plasma is discharging into air with flat profiles at inlet: a mean value of velocity is derived from the mean value of mass flow rate which is experimentally known, and a mean value of temperature is derived from the mean value of enthalpy calculated from the plasma characteristics.

Several turbulence models proposed in FLUENT are compared with these conditions: the Realizable k-epsilon model with standard constant proposed in ANSYS Fluent, the standard k-epsilon, as well as the SST-k-omega model (that was also implemented to overcome the problems of k-epsilon and k-omega models) and the k-omega model for comparison purposes.

Figure 2 and Figure 3 below present the temperature and velocity magnitudes of the free jet with the realizable and standard k-epsilon model tested in FLUENT.
The hot plasma gas is injected from the bottom left side of the mesh, and exits from the tubular canal into the ambient air. Cold air is injected from the left side at low velocity and room temperature. The gas mix exits the simulation box through a pressure outlet on the right side of the simulation box.

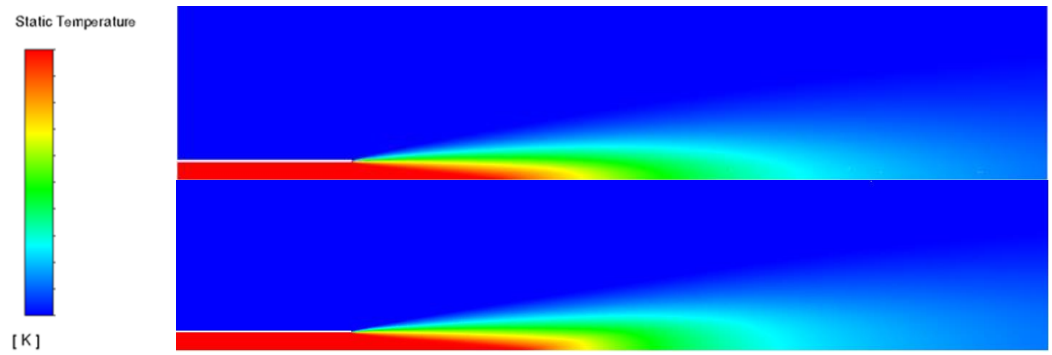

Figure 2 : Fields of temperature of the free stream jet simulate in Fluent with flat profile inlet assumptions, with realizable k-epsilon model (above) and standard k-epsilon model (below).

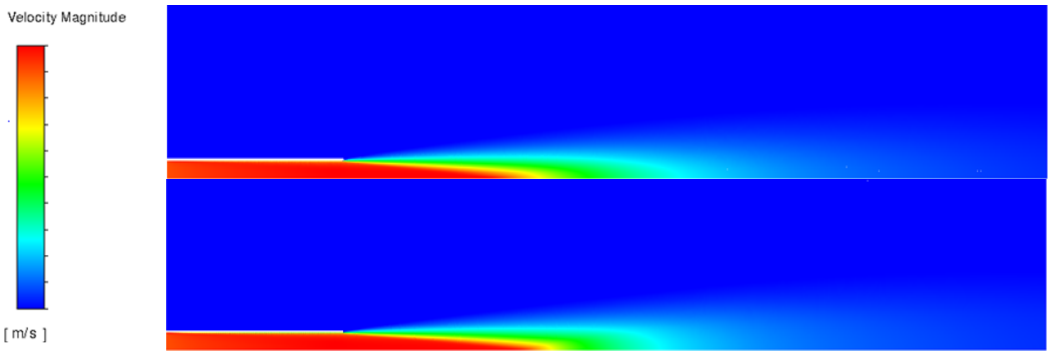

Figure 3 : Fields of velocity of the free stream jet simulate in Fluent with flat profile inlet assumptions, with realizable k-epsilon model (above) and standard k-epsilon model (below).

As observed on the figures above, the temperature and velocity fields have rather similar appearances between the two turbulence models. Additional post-treatments of the simulated jet is necessary to highlight the differences between them.

Figure 3 and Figure 4 below present the temperature and velocity axial profiles of the round free jet along its symmetry axis x. Negative values of x are inside the tubular canal, the position x=0 corresponds to the exit section of the tubular canal, and positive values of x correspond to the external jet. The latter is composed of two distinct regions from left

DOI: 10.13009/EUCASS2023-807

to right: first, the high-energy potential core, where the central values of velocity and temperature remain constant along the symmetry axis until a certain distance, then, the interfacial intermediate region, where temperature and velocity profiles start dropping due to jet expansion and progressive turbulent mixing with the cold ambient gas along the axis, causing an attenuation of the jet that stabilizes at long distances from the exit.

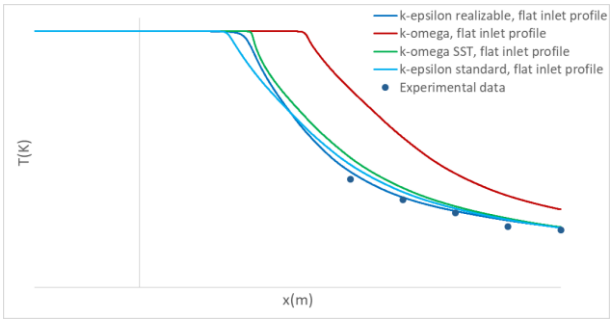

Figure 4: Temperature profiles along the central axis x with assumptions of flat profiles inlet for different turbulence models

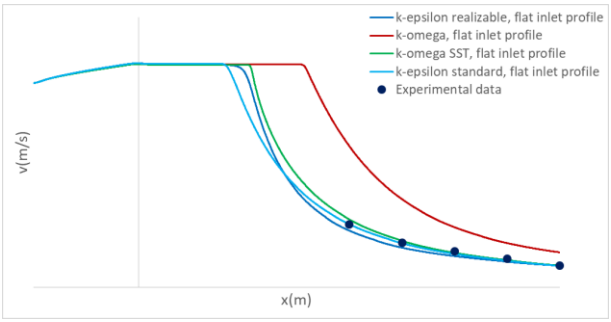

Figure 5: Temperature profiles along the central axis x with assumptions of flat profiles inlet for different turbulence models

The Realizable k-epsilon, the standard k-epsilon and the SST k-omega models give overall similar results in terms of potential core length and decrease rates in the interfacial regions close to the potential core, despite minor differences that will be discussed below. Besides, all three models stabilize away from the torch exit toward similar temperature and velocity values, and comply with the experimental measurements in the far field. Based on these observations, all three models seem appropriate for this round torch jet simulation so far.
In comparison, the standard k-omega model differs from the other three by a much longer potential core and a much slower decrease rate in the intermediate region. In addition, it tends towards significantly higher values temperature and velocity stabilization values which are not in agreement with the experimental data. The standard k-omega model was only tested here for comparison purposes as it is well known to perform poorly in free stream regions. These observations confirm that the standard k-omega model is not appropriate for this round jet torch simulation.

For the other three models, some less significant differences can be observed.

The realizable k-epsilon model shows a longer potential core and a faster attenuation rate in the intermediate zone compared to the standard k-epsilon model in this simulation. As this model it has been originally proposed to overcome some well-known limitations of the standard k-epsilon model with regard to jet attenuation, it can be assumed that the central profiles obtained with realizable k-epsilon in this simulation are more realistic at this point.

Realizable k-epsilon and SST k-omega are quite similar in terms of potential core length. The former has a faster decay rate out of the potential core, but both end up stabilizing toward similar values, as described above.

SST k-omega model has an intermediate behaviour between standard k-epsilon and standard k-omega. This observation supports the usual statement that SST k-omega model combines the advantages of k-omega models near the walls and those of k-epsilon models in the free stream. The cooled torch exit canal being included in the simulation, it is reasonable to assume that near-wall performances of the chosen turbulence model will also play a role in the overall accuracy of the CFD simulation; however, as k-omega SST is closer to standard k-epsilon than to standard k-omega in this simulation in terms of calculated profiles, it seems that the free stream and turbulence mixing effects are predominant with regard to the near-wall effects of the torch canal.

At this point in the analysis, Realizable and standard k-epsilon, as well as SST k-omega turbulent models all seem to be appropriate to this round plasma jet simulation, as opposed to the standard k-omega model.

However, it has to be noted that those simulations were carried out as a first approximation with an unrealistic flat inlet profile hypothesis. This modelling choice tends to distort particularly the maximum speed and maximum temperature values at the centre of the jet in the simulation, and thus, affects the representativeness of the simulated jet close to the torch exit.

DOI: 10.13009/EUCASS2023-807

Therefore, in the following section, similar simulations will be performed with more realistic assumptions of temperature and velocity profiles at the hot plasma boundary inlet.

4.2 Free jet simulations with velocity and temperature profiles at the inlet boundary of the torch

The free jet simulations are then improved by adding more realistic forms of velocity and temperature profiles at the inlet boundary. As reminded by Bolot ([21]), profiles at a torch exit are often expressed in literature with the following expressions:

- $v(r) = v_{axis}\left(1 - \left(\frac{r}{R}\right)^{n_v}\right)$ for velocity profile
- $h(r) = h_{bc}\left(1 - \left(\frac{r}{R}\right)^{n_h}\right)$ for enthalpy profile (which can also be derived in terms of temperature)

For convenience reasons, in this paper, the second equation will be expressed in terms of temperature rather than enthalpy. On the outer wall of the torch, the temperature is imposed by the cooling system of the torch to a constant value T_w, and the velocity is assumed to be zero, which leads to :

$$T(r) = T_w + T_{axis}\left(1 - \left(\frac{r}{R}\right)^{n_T}\right)$$

Many values of exponent coefficient n_v and n_h (or n_T) can be found in literature. The coefficient are arbitrarily chosen equal to the one of the multiple combinations proposed by Bolot ([21]), $n_v = 2$ and $n_T = 4{,}5$. As explained by Bolot, even in the case where velocity and enthalpy profiles have the same exponents ($n_v = n_h$), the temperature profiles tend to have a higher exponents than the velocity profiles, and therefore become more flat. This is due to the fact that in the high temperature range of a plasma torch, at the exit, the gas field is still partially ionized and the heat capacity increases with temperature. Then, near the central axis where temperature is at its maximum, a given variation of enthalpy gives a smaller variation of temperature. The profiles are chosen so that the mean values of velocity and temperature are similar the flat profile cases seen before.

Figure 6 and Figure 7 below presents the temperature and velocity axial profiles of the free jet with these new assumptions of inlet profiles, compared to the results previously obtained with assumptions of flat inlet profiles.

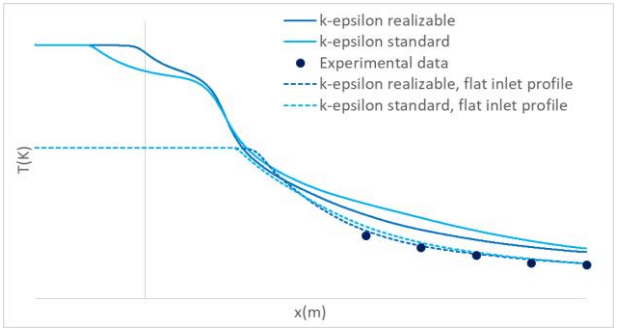

Figure 6: Temperature profiles along the central axis x with a hypothesis of profile inlet for different turbulence models (bold lines: realistic profiles at inlet, dotted lines: flat profiles at inlet)

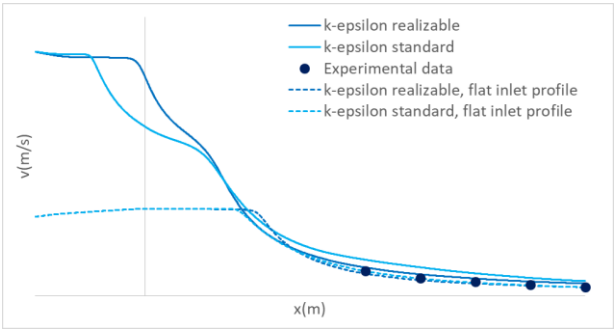

Figure 7: Temperature profiles along the central axis x with a hypothesis of profile inlet for different turbulence models (bold lines: realistic profiles at inlet, dotted lines: flat profiles at inlet)

The comparisons between Realizable and standard k-epsilon made in the previous section are still valid with these new inlet assumptions.

Despite having much higher maximum values of velocity and temperature at the center of the hot inlet, the temperature and velocity profiles calculated along the central line with these new assumptions rapidly decrease and end up joining the results generated in the previous sections (with flat inlet profiles assumptions) right after the potential core of the former. However, the choice of the profiles of velocity and temperature at inlet still has a noticeable impact

DOI: 10.13009/EUCASS2023-807

on the free stream of the jet even at a 3 or 4-potential length distance after the exit, as the jet injected with higher central values at inlet tend to remain hotter and faster in the distance than the one injected with flat profiles with lower central values of temperature and velocities.

With these new inlet conditions, the calculated profiles can also be compared with velocity and temperature measurement along the axis. The realizable k-epsilon model tends to give lower temperature and velocity than the standard k-epsilon one at long distances, and hence to be more consistent with experimental data in this region, which tends to demonstrate its ability to improve jet attenuation and mixing effects simulations. However, these data suggest that the jet attenuation calculated in this simulation may still not be strong enough with regard to experimental data. This matter is addressed in the following section.

It can also be noted that for the first type of boundary conditions, with flat profiles of temperature and velocity at the exit of the torch, the jet remains subsonic, while for the second type of boundary conditions, the jet is supersonic inside the tubular canal. The latter then rapidly becomes subsonic after the exit of the torch. In both simulations, Mach number was found to be close to 1 (either slightly lower or slightly higher than 1 respectively). From these two examples, it can be assumed that there are several other combinations of parameters (T_{axis}, v_{axis}, n_T, n_v) which would allow the external plasma jet to be simulated correctly in terms of average enthalpy, average mass flow rate and axial attenuation profile along the central axis (away from the potential core), in accordance with experimental data. The simulated jet would then probably has either slightly subsonic or slightly supersonic behaviour. Based on experimental observations, the external jet is rather supposed to remain subsonic.

4.3 Jet simulation with a heat probe exposed to the flux.

The second configuration to be modelled in CFD is a calibration test performed by exposing a heat probe into the plasma jet.

The distance D between the probe and the torch exit from the exit was calibrated to ensure that the probe would remain outside of the potential core so that the heat flux seen by the probe would remain below its maximum specification (5MW/m^2).

This test was performed to calibrate the heat flux seen by a real sample of composite material during an ablation test. Therefore, the heat probe carrier was built with the same specific design as the sample carrier used for ablation test campaigns: its shape is intended to generate controlled convection and shear conditions at the surface of the sample, which are of prime importance for ablation studies on composite material, as described previously in the introduction, due to the predominant competition between oxidation, diffusion and mechanical effects in composite ablation problems.

The CFD mesh was rebuild in 3D in order to include the geometry of this non-asymmetrical probe carrier device. The temperature and velocity fields around the heat probe are shown in Figure 8 and Figure 9 below, but for confidentiality purpose, the exact probe geometry is masked in these figures.

The temperature at the surface of the heat probe is experimentally controlled by its own cooling system. Therefore, in the simulation, a value of surface temperature is imposed as a boundary condition at the wall representing the heat probe surface in the CFD simulation.

As the physics is getting more complex, the Realizable k-epsilon model is preferred to the standard k-epsilon model as it has showed improved results on many physical problems, including prediction of round jets dissipation rates. The Realizable model is coupled with a wall treatment option ensuring good accuracy of the boundary layer and thermal effects near the probe.

DOI: 10.13009/EUCASS2023-807

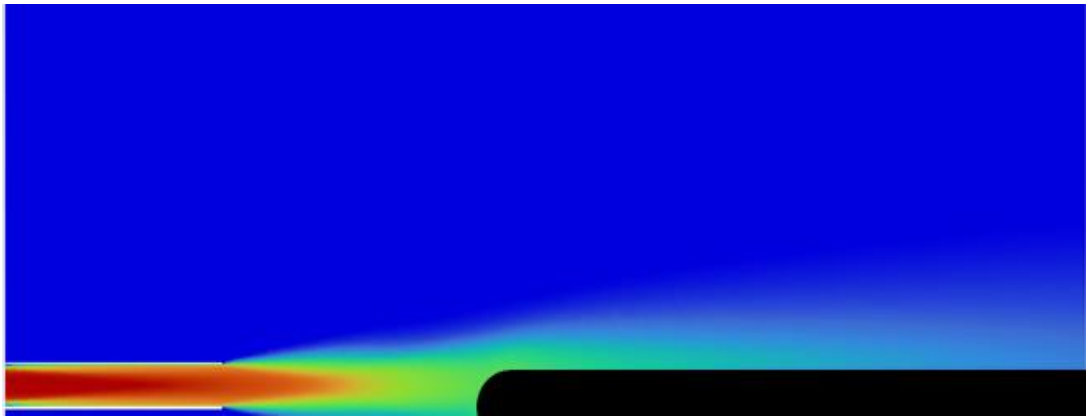

Figure 8 : Temperature field around the heat probe exposed to the external plasma jet

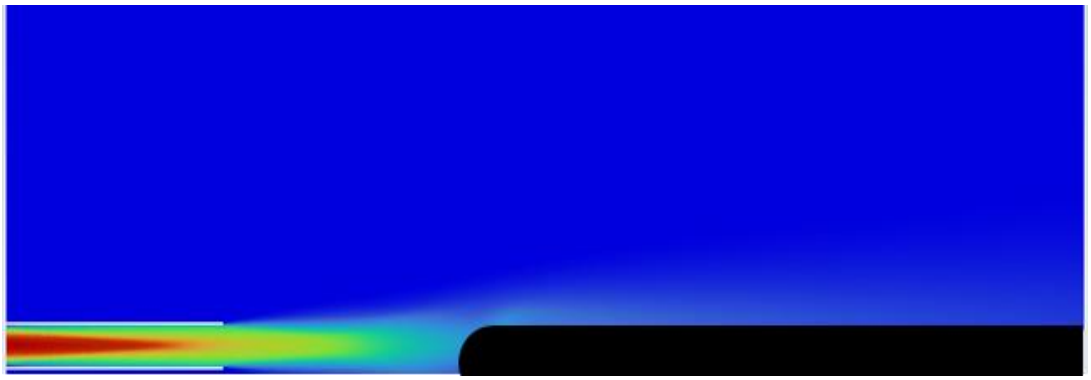

Figure 9 : Velocity field around the heat probe exposed to the external plasma jet

In the previous sections, it has been showed that the jet attenuation needed to be accentuated in this simulation. Therefore, new sets of constant have been tested for the heat probe 3D CFD simulation with realizable k-epsilon model. The C2-epsilon coefficient was increased by a few percent, in order to increase the turbulent dissipation rate, and C1-epsilon was adjusted accordingly according to Turpin and Troyes ([9]). Apart from the reference simulation with standard values of C2-epsilon and C1-epsilon constants (simulation 0), three other simulations (n°1, 2 and 3) were performed with a multiplying coefficient $(1 + \varepsilon_i)$ applied to the standard C2-epsilon value in the dissipation rate equation (with $\varepsilon_i > 0$ for $i \in [1,2,3]$ and $\varepsilon_1 < \varepsilon_2 < \varepsilon_3$).

The heat flux calculated at the heat probe surface was then compared to the value obtained experimentally as shown in Table 1:

Table 1 : Mean value of heat flux simulated on the heat probe exposed to the plasma jet with k-epsilon realizable model compared to the experimental measurement

Simulation	Coefficient of the C2-epsilon constant	Heat Flux (MW/m^2)	Relative difference with experimental measure
0	1	2,83	62%
1	$(1 + \varepsilon_1)$	2,35	34%
2	$(1 + \varepsilon_2)$	1,78	2%
3	$(1 + \varepsilon_3)$	1,90	9%
Experimental measure		1,75	

Simulation n°2 matches pretty well with the experimental measurement with a 2% error. Simulation n°3 also gives a reasonably accurate value of mean heat flux with a 9% relative difference with the experimental value. Although this

DOI: 10.13009/EUCASS2023-807

set of constants provides the correct results of heat fluxes in this precise case, it cannot be generalized; a part of the adjustment of C1-epsilon and C2-epsilon constants in the realizable k-epsilon model are probably very dependent on the simulation conditions and simplifications decided at the beginning of this analysis. This new set of parameters should be tested for different distances between the heat probe and the torch exit in order to verify that it could also be used in more generalized configurations.

The velocity and temperature profiles of free stream plasma jet (without the heat probe design) calculated with the two sets of parameters validated above (n°2 and n°3) are compared to the results calculated previously, for comparison and illustration purposes.

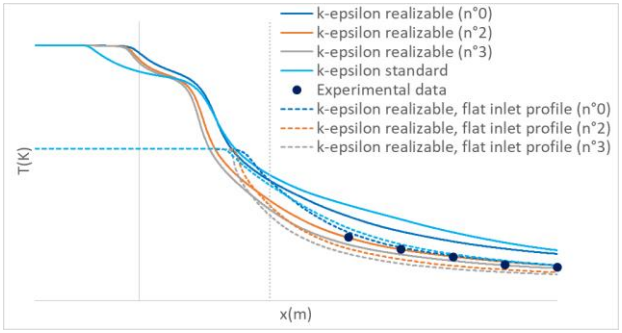

Figure 10: Temperature profiles along the central axis x with two hypotheses of profile inlet and different turbulence models including Realizable k-epsilon with modified sets of constants

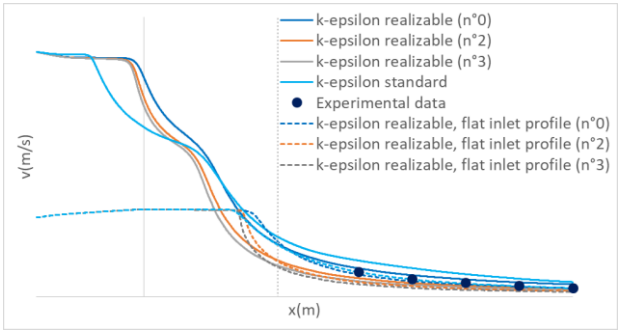

Figure 11: Velocity profiles along the central axis x with two hypotheses of profile inlet and different turbulence models including Realizable k-epsilon with modified sets of constants

4.4. Analysis of the flow inside the potential core

Inside the potential core, the extreme conditions make any direct experimental measurement impossible, unless for sacrificial tests (such as ablation tests were the samples of composite material are not meant to be reused).

To overcome this lack of experimental data in the potential core, data from an ablation tests performed on similar samples (made of a reference high-performance, ablation-resistant Ceramic Matrix Composite material), are used to provide estimations of the flow characteristics in this area.

During these ablation tests, the temperatures at the surface of the samples were measured by pyrometers and a spectroradiometer. Besides, thermocouples were placed inside of the sample to monitor the evolution of in-depth temperature.

The thermal properties, heat capacity C_p and thermal conductivity k, are known from previous material characterizations, and expressed as functions of temperature: $C_p(T), k(T)$. The density ρ of the material is also known. A one-dimensional thermal simulation is performed with a thermal conduction code (MARC), solving heat equation:

$$\rho C_p \frac{\partial T}{\partial t} - k\nabla T = S$$

With S the volumetric heat source term.

According to [22], [23], the energy balance at the ablating surface exposed to the plasma environment simplifies to:

$$q_{diff} + q_{rad,in} - q_{rad,out} - (\rho v)h_w + \dot{m}_s h_s = q_{cond}$$

Where:

DOI: 10.13009/EUCASS2023-807

- q_{diff} (also known as q_{conv} in some papers) accounts for all diffusive energy fluxes from the gas boundary layer (either from heat conduction due to a temperature gradient in the gas adjacent to the wall or energy convected to the surface as a result exothermic or endothermic chemical reactions).
- $q_{rad,in}$ and $q_{rad,out}$ are incident radiation flux and re-radiation flux from the surface respectively, with $q_{rad,out} = \sigma\epsilon T_w^4$
- $(\rho v)h_w$ is the energy flux leaving the surface with the "blowing flux" $(\rho v)_w$ from the wall
- $\dot{m}_s h_s$ is the energy flux associated with surface ablation.

As a first rough approximation, the energy balance equation is simplified as if all terms linked to loss of mass from the material (blowing and ablation) could be neglected for this Ceramic Matrix Composite since this material is highly resistant to ablation (although not fully resistant). For simplification purposes, gaseous species in the oxidizing flow are assumed to have the same diffusion coefficients, and Lewis and Prandtl coefficients are supposed equal to unity. The diffusive term and the conservation energy then simplify to:

$$q_{diff} = q_{conv} = h\left(T_{gas} - T_w\right)$$
$$h(T_e - T_w) + q_{rad,in} - \sigma\epsilon T_w^4 = q_{cond}$$

T_e and T_w are the temperatures at the edge of the boundary layer and at the wall respectively, and h is a convective coefficient given by boundary layer calculations. The external gas temperature at the boundary layer edge T_e is considered constant in this simulation, whereas the wall temperature T_w is a function of time in this unsteady thermal simulation ($T_w(t)$). The surface and in-depth material temperatures are expected to increase and stabilize towards a stabilization values as a results of the constant incident energy fluxes imposed in the simulation.

The convective flux can also be expressed as a function of the reference convective flux at 300K, $q_{conv,300K}$:

$$q_{conv} = q_{conv,300K}\frac{(T_e - T_w)}{(T_e - 300)}$$

Then:

$$q_{conv,300K}\frac{(T_e - T_w)}{(T_e - 300)} + q_{rad,in} - \sigma\epsilon T_w^4 = q_{cond}$$

The incident radiative flux $q_{rad,in}$ is calculated under the approximation that the plasma is transparent, and is considered constant during the duration of the experiment.

A parametrical study was performed with the following variables for the energy balance equation at the surface:

- The material emissivity within the range of possible values known for the material tested $[\epsilon_{min}, \epsilon_{max}]$
- The hot gas (plasma) temperature in the potential core at the center of the jet within the range [4500K, 6500K]
- The reference convective heat flux at 300K $q_{conv,300K}$ within the range [6MW/m^2, 8MW/m^2]

Figure 12 below presents a comparison between the spectroradiometer measurements and the calculated surface temperature.

Figure 13 below presents a comparison between the thermocouple measurements inside the sample and the calculated temperatures at the same depth under the ablative surface.

DOI: 10.13009/EUCASS2023-807

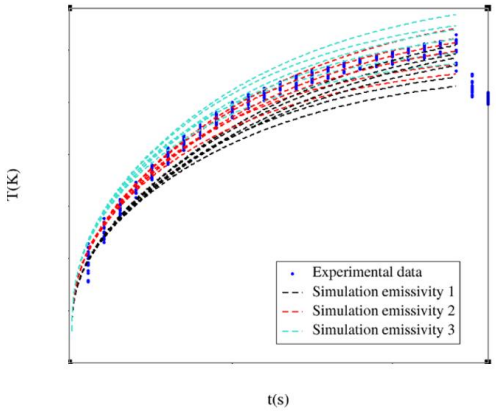

Figure 12: Surface temperature calculated with different sets of parameters (regarding the energy balance equation at the surface) compared to spectroradiometer measurements during an ablation test on a CMC sample.

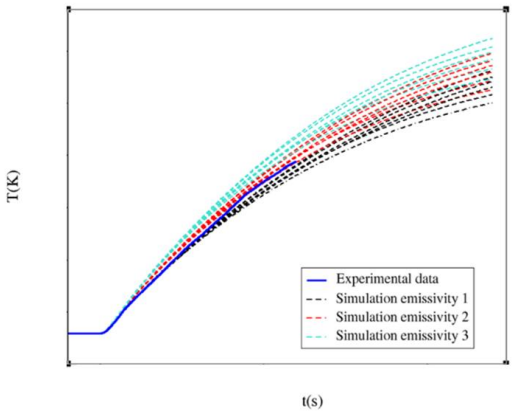

Figure 13 : In-depth temperature calculated with different sets of parameters (regarding the energy balance equation at the surface) compared to the thermocouple measurements during an ablation test on a CMC sample.

With these approximations, it is found that a convective heat flux in the potential core with a convective heat flux at 300K $\Phi_{conv,300K}$ of about 6 to 8 MW/m^2 and gas temperature of about 4500-6500K are still consistent with spectroradiometers temperature measurements. Due to uncertainties regarding the exact values of surface emissivity of the sample material, several combinations of parameters are still acceptable at this point to characterize the plasma jet external flow around the heat probe in this experiment.

This concludes the calibration of the aerodynamics contribution to the model.

It should be noted that this analysis, which neglects ablation and material degradation, allows only a rough estimation of the orders of quantities involved. For instance, the simulated temperature does not follow exactly the same trend as the experimental measurements, whose temperatures rise faster in the first half of the test but then also stabilize more efficiently in the second half of the test. It may suggest the following pattern regarding ablation rate at the surface of the sample: in the first part of the test, the ablation rate is limited by reaction and increases progressively with the material surface temperature; then, in the second part of the test, the oxidation rate becomes limited by diffusion and reaches a maximum constant value; then, as the hot surface layers of the material are quickly removed from the surface of the sample by ablation, this may help stabilize the sample surface temperature, which is also led by in-depth thermal conduction through the sample material.
This kind of scenarios will have to be confirmed by further analysis, and the energy balance equation will then have to be refined. In particular, surface energy losses due to material degradation will have to be considered in order to better reproduce fluid-solid interactions during the test.

5. Conclusion

The external thermal plasma jet of the air plasma torch operated by ArianeGroup can be modelled with an acceptable accuracy along the central axis outside of the potential core, with means of CFD simulations using conventional turbulence models such as the realizable k-epsilon model, which, as expected, is showing better performances to simulate the attenuation of the round plasma jet than the standard k-epsilon model.
One of the difficulties in modelling external plasma jets is that the velocity and temperature profiles of the external jet releasing into ambient air are unknown and cannot be measured experimentally. Some assumptions then have to be made regarding the input profiles, which, on the one hand, tend to have a small influence in the intermediate region of the jet, away from the torch exit, but on the other hand strongly impact the flow, speed and temperature levels near the jet outlet in the potential core, especially along the central axis. These uncertainties have to be taken into account when modelling plasma jet ablation tests.
Regarding the accuracy of the realizable k-epsilon model with regards to the experimental flow measurements, adjustments of the constants C2-epsilon and C1-epsilon were necessary to correctly reproduce the measured flows by influencing the rate of turbulent dissipation in the simulation. The new sets of constants tested for this matter are though

DOI: 10.13009/EUCASS2023-807

probably dependent on the assumptions taken for this simulation, and may be tested over different distances to check their validity domain. Finally, for areas where classic experimental data are not available, such as into the potential core, temperatures measurements during ablation tests may be used. A simplified flow balance is able to confirm the orders of heat flux quantities in the potential core of the jet. The model will now have to be refined by including modelling of ablation equations. The long term objective is to build a completely coupled fluid-solid simulation reproducing the behaviour of a composite material under the air plasma torch operating conditions, in the context of material screening application.

6. Acknowledgments

The authors would like to thank Dr Julien Richard from ArianeGroup for helpful discussions.

7. References

[1] Takali, S. C. 2015. Modélisation CFD de l'écoulement dans une torche plasma triphasée de 100kW fonctionnant à l'air. Influence du rayonnement de l'arc.
[2] Xiong H.B., Zheng L.L., Sampath S., Williamson R.L., Fincke J.R., 2004, Three-dimensional simulation of plasma sparay: effects of carrier gas flow and particle injection on plasma jet and entrained particle behaviour, *International Journal of Heat and Mass Transfer 47, 5189-5200*.
[3] Shigeta, M. 2018. Modeling and Simulation of a turbulent-like Thermal Plasma Jet for Nanopowder Production.
[4] Launder B.E. & Spalding D.B., 1972, Lectures in Mathematical Models of Turbulence, *Academic Press, London, England.*
[5] Launder B. E. et al, 1972. The prediction of free shear flows - A comparison of six turbulence models. *NASA SP-311*.
[6] McGuirk J.J. & Rodi. W. 1977. The calculation of three dimensional free jets. *Symposium on turbulent shear flows, Pennsylvania State University*.
[7] Morse A.P., 1972. Axisymetric turbulent shear flows with and without swirl. *PhD Thesis, London University*.
[8] Pope S. B., 1978. An explanation of the turbulent round-jet/plane anomaly. FS 77/12, *Imperial College of Science and Tehcnology*.
[9] Turpin G. & Troyes J., 2000. Validation of a two-equation turbulence model for axisymmetric reacting and non-reacting flows. *36th AIAA/ASME/SAE/ASEE Joint propulsion Conference and Exhibit Huntsville. AL (USA), July 16-19, 2000*.
[10] Bolot R., et al. 2004. Modeling of thermal plasma jets : a comparison between PHOENICS and FLUENT. *LERMPS-UTBM, Belfort /F*.
[11] Zhang Haiou et al. (2006). Modeling and simulation of a plasma jet by Lattice Boltzman method.
[12] Shih T.-H., et al. 1994. A New k-epsilon Eddy Viscosity Model for High Reynolds Number Turbulent Flows - Model Developement and Validation. *NASA Technical Memorandum 106721*.
[13] Levet C., et al. 2016, Microstructure and gas-surface inetraction studies of a 3D carbon/Carbon composite in atmospheric entry plasma, *Carbon*.
[14] Turchi A., et al., 2017, Thermochemical ablation modeling forward uncertainty analysis – Part II : Application to plasma wind tunnel testing, *International Journal of Thermal Science*.
[15] Ulh J. et al., 2010, Pyrolysis Simulation in an ICP Torch Facility, *42nd AIAA Thermophysics Conference, 27-30 June 2011*
[16] Williams F.A., 1985, Combustion Theory, *Benjamin/Cummings, Menlo Park, California*
[17] Williamson R.L. et al. (2002). Entrainment in high-velocity, high temperature plasma jets, Part II : computational resultats and comparison to experiment, *International Journal of Heat and Mass Transfer, Volume 46, Issue 22, October 2003, Pages 4115-4228.*
[18] Fincke J.R. et al. 2003, Entrainment in high-velocity, high-temperature plasma jets. Part I : experimental results
[19] Chaplygin A, Combined Surface Heating by Laser Beam and Subsonic Nitrogen Plasma Jet, *International Journal of Heat and Mass Transfer, Volume 46, Issue 22, October 2003, Pages 4201-4213.*
[20] Ramshaw J.D. & Chang C.H., Computationnal fluid dynamics of multicomponent thermal plasmas, *Plasma Chem. Plasma Process, 12 (1992) 299-325.*
[21] Bolot, 1999, Modélisation des écoulements de plasmas d'arc soufflé : Application à la projection de matériaux pulvérulents. *PhD Thesis, Université de Franche-Comté*
[22] Moyer C.B., 1968, Rindal R. A., An analysis of the coupled chemically reacting boundary layer and charring ablator, *NASA.*
[23] Schoner R., Aerotherm Graphite Surface Kinetics Computer Program, Volume I – Problem description and sample models

DOI: 10.13009/EUCASS2023-807

Appendix: Turbulence models

In k-epsilon models, k is the kinetic energy of mean turbulent movement, defined by; $k = \frac{1}{2}u_i u_i$ and ϵ is the rate of dissipation of kinetic energy defined by: $\rho\epsilon = \mu\frac{\partial u_i}{\partial x_j}\frac{\partial u_i}{\partial x_j}$.

The equations of standard k-epsilon models are the following:

- A transport equation of turbulent kinetic energy k is the same for both standard and Realizable k-epsilon models :

$$\frac{\partial(\rho k)}{\partial t} + \frac{\partial(\rho k u_i)}{\partial x_i} = \frac{\partial y}{\partial x_i}\left[\left(\mu + \frac{\mu_t}{\sigma_k}\right)\frac{\partial k}{\partial x_j}\right] + P_k - \rho\epsilon + S_k$$

With $P_k = (G_k + G_b - Ym)$ in Fluent model.

Where G_k is the generation of turbulence kinetic energy due to the mean velocity gradient, G_b is the generation of kinetic energy due to buoyancy, Y_m is the contribution of the fluctuating dilatation in compressible turbulence to the overall dissipation rate, σ_k and σ_ϵ are the turbulent Prandtl numbers for k and epsilon. And S_k and S_ϵ are user-defined source terms.

- A transport equation of ϵ (also known as the dissipation rate equation) is different between the two models :

$$\frac{\partial}{\partial t}(\rho\epsilon) + \frac{\partial}{\partial x_j}(\rho\epsilon u_j) = \frac{\partial}{\partial x_j}\left(\left(\mu + \frac{\mu_t}{\sigma_\epsilon}\right)\frac{\partial \epsilon}{\partial x_j}\right) + C_{1\epsilon}\frac{\epsilon}{k}(G_k + C_{3\epsilon}G_b) - \rho C_{2\epsilon}\frac{\epsilon^2}{k} + S_\epsilon$$

In the realizable k-epsilon model, the second equation is modified;

$$\frac{\partial}{\partial t}(\rho\epsilon) + \frac{\partial}{\partial x_j}(\rho\epsilon u_j) = \frac{\partial}{\partial x_j}\left(\left(\mu + \frac{\mu_t}{\sigma_\epsilon}\right)\frac{\partial \epsilon}{\partial x_j}\right) + C_{1\epsilon}\frac{\epsilon}{k}C_{3\epsilon}G_b - \rho C_{2\epsilon}\frac{\epsilon^2}{k+\sqrt{\nu\epsilon}} + S_\epsilon(1 + \rho C_{1\epsilon})$$

The turbulent (or eddy) viscosity is defined by $\mu_t = \frac{\rho C_\mu k^2}{\epsilon}$.

- In the standard k-epsilon model, the dynamic viscosity coefficient C_μ is a constant for the standard k-epsilon model with constant values: $C_{1,\epsilon} = 1{,}44$, $C_{1,\epsilon} = 1{,}92$, $C_\mu = 0{,}09$, $\sigma_k = 1{,}0$ and $\sigma_\epsilon = 1{,}3$.
- In the Realizable k-epsilon model, a new formula of the eddy viscosity $\mu_t$is proposed with $C_\mu$being a function of the mean strain and rotational rates , the angular velocity of the system rotation and the turbulence fields k and epsilon :

$C_\mu = \frac{1}{A_0 + \frac{A_S k U^*}{\epsilon}}$ with $U^* \equiv \sqrt{S_{ij}S_{ij} + \widetilde{\Omega_{ij}}\widetilde{\Omega_{ij}}}$ and $\widetilde{\Omega_{ij}} = \Omega_{ij} - 2\epsilon_{ijk}\omega_k$ and $\Omega_{ij} = \overline{\Omega_{ij}} - \epsilon_{ijk}\omega_k$